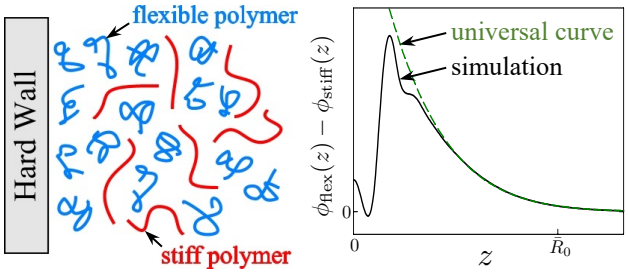
Universality of Entropic Surface Segregation from Athermal Polymer Blends Due to Conformational Asymmetry

Russell K. W. Spencer*,† and Mark W. Matsen*,‡

†*Institut für Theoretische Physik, Georg-August Universität, Friedrich-Hund-Platz 1, 37077 Göttingen, Germany*

‡*Department of Chemical Engineering, Department of Physics & Astronomy, and Waterloo Institute for Nanotechnology, University of Waterloo, Waterloo, Ontario N2L 3G1, Canada*

E-mail: russell.spencer@uni-goettingen.de; mwmatsen@uwaterloo.ca



Abstract

We reexamine off-lattice Monte Carlo simulations for athermal blends of stiff and flexible polymers next to a hard wall. The original simulations [Kumar et al., *J. Chem. Phys.* **1995**, *103*, 10332], which were supported by wall-PRISM calculations, predicted a short-range preference for the stiff polymers at the wall, which contradicts experiments as well as alternative calculations. On this basis, Kumar et al. asserted that the true entropic preference in the experiments was masked by enthalpic interactions, and that the other calculations were incorrect because they did not account for local packing effects at the wall. However, with vastly improved equilibration and statistics, we now find that the simulations actually predict a long-range surface preference for the flexible polymers, which resolves a controversy that has existed for over 25 years. Furthermore, we show that the excess of flexible polymer adopts a universal concentration profile, as predicted by mean-field theory [Wu et al., *J. Chem. Phys.* **1996**, *104*, 6387].

Introduction

The blending of polymers provides a simple means of tailoring material properties. However, it can also complicate surface properties, which are important for many technological applications including adhesion, lubrication, wetting, colloidal stabilization, catalysis, material processing, and protein adsorption.[1] Naturally, surface behavior will generally depend on both enthalpic and entropic effects, but it is usually the enthalpy that dominates. As a result, the role of entropy has received less attention. It is, nevertheless, well understood that entropy favors small polymers at the surface, as confirmed by theory,[2–4] simulations,[5] and experiments.[6] On the other hand, researchers have yet to develop a consistent understanding of entropic surface segregation due to conformational asymmetry.

The effect of conformational asymmetry was first noticed by Sikka et al.[7,8] in experiments on a series of polyolefin diblock copolymers, where the two components were chemically similar but with considerably different statistical segment lengths. Note that the comparison is based on segments of equal molecular volume. The experiments observed that the diblock copolymers always ordered with the short-segment-length component at surfaces. Subsequent experiments by Scheffold et al.[9] on binary polyolefin blends also found similar preferences. Other experiments by Tretinnikov and Ohta[10,11] examined blends of isotactic and syndiotactic PMMA, where the monomers of the two polymers are identical but linked together differently resulting in a shorter statistical segment length for the syndiotactic version. Again, it was the short-segment-length component that segregated to surfaces. Despite the chemical similarity of the components, it is still uncertain whether or not the experiments were truly free of significant enthalpic effects.[9–11]

Theories have the distinct advantage that they can ensure there is no enthalpic bias, but despite this advantage they have actually confused the issue. Density functional theories (DFTs)[12,13] and self-consistent field theory (SCFT)[14,15] have predicted that the polymers with the shorter statistical segment length segregate to the surface. However, wall-PRISM calculations[16,17] predicted the opposite. Likewise, Stepanow and Fedorenko[18] found that

fluctuation corrections to SCFT lead to a preference for the component with the longer statistical segment length.

Simulations provide a means of testing the approximations used by theories, but this too has not resolved the contradictory results. Monte Carlo (MC) simulations by Kumar and coworkers[16,17] of binary blends of flexible and stiff polymers next to hard walls observed a general preference for the stiff polymers with the longer statistical segment length, which quantitatively supported the wall-PRISM calculations. On the other hand, molecular dynamics (MD) simulations on diblock copolymer melts by Nikoubashman et al.[19] reported a preference for the component with the shorter statistical segment length. Most recently, we performed MC simulations of flexible and stiff polymers,[20] and found a general preference for the flexible polymer, quantitatively consistent with the SCFT calculations of Wu et al.[15]

Despite their diametrically opposing conclusions, the only meaningful difference between the simulations of Kumar and coworkers[16,17] and our previous ones[20] is that they are based on off-lattice and lattice models, respectively. It is a common practice to restrict the monomers of large and relatively flexible polymers to a lattice so as to increase the computational efficiency of simulations, with the expectation that the artificial lattice will not alter the qualitative behavior.[21,22] If the lattice does actually reverse the surface segregation, then one also needs to consider the possibility that the behavior is hypersensitive to model details, implying the potential need for accurate models involving atomistic details. This possibility is actually supported by similar off-lattice simulations[23] for blends of linear and branched polymers, which found that the segregation was sensitive to the details of the interactions with the walls and between monomers. Another, perhaps more palatable, possibility is that the earlier and more computationally challenging off-lattice simulations may have been corrupted by non-equilibrium effects. Indeed, there exist serious irregularities in their reported radii of gyration, and furthermore their protocol for equilibration appears inadequate as we will discuss shortly. Given these concerns and the potential ramifications, we reexamine the off-lattice MC simulations.

Monte Carlo Simulation

The simulations involve n polymers of which n_s are stiff and $n_f = n - n_s$ are flexible. The stiff polymers are labeled by $j = 1, 2, ..., n_s$ and the flexible polymers by $j = n_s + 1, n_s + 2, ..., n$. To avoid entropic segregation due to size disparity,[2–6] both polymers have an equal number of monomers labeled by $i = 1, 2, 3, ..., N$. The vector $\mathbf{r}_i^{(j)}$ denotes the center of monomer i of polymer j, as depicted in Figure 1. Monomers are treated as impenetrable spheres of diameter one, which defines our length scale, and polymers are modeled as tangent spheres, which is enforced by restricting the bond vectors, $\mathbf{u}_i^{(j)} \equiv \mathbf{r}_{i+1}^{(j)} - \mathbf{r}_i^{(j)}$, to a length of one, as depicted in Figure 1. The conformational asymmetry is introduced by applying a bending energy of

$$\frac{E_{\text{bend}}}{k_B T} = -\kappa \sum_{j=1}^{n_s} \sum_{i=1}^{N-1} \mathbf{u}_i^{(j)} \cdot \mathbf{u}_{i+1}^{(j)} \tag{1}$$

to the stiff polymers where κ is a dimensionless bending modulus. The polymers are placed in a simulation box of size $L_x \times L_y \times L_z$ and volume $V = L_x L_y L_z$ with periodic boundaries in the x- and y-directions and impenetrable walls at $z = 0$ and L_z. In all cases, we fill the simulation box to an average monomer concentration of $nN/V = 0.6$, a value regarded by Kumar et al.[17] as corresponding to melt density.

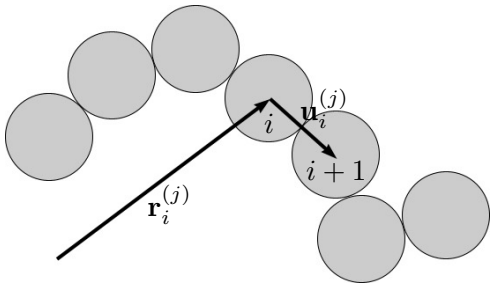


Figure 1: Illustration showing a portion of the jth polymer. The position of the ith monomer is denoted by the vector $\mathbf{r}_i^{(j)}$ and the orientation of its bond with the $(i+1)$th monomer is denoted by the unit vector $\mathbf{u}_i^{(j)}$.

Our MC simulations attempt, with equal probability, reptation, end-rotation, crankshaft, and swap trial moves; the first three single-chain moves are illustrated in Figure 2. Each trial

is immediately rejected if it results in an overlap, and otherwise it is accepted or rejected based on the standard Metropolis criterion. The reptation trial randomly selects one of the $2n$ end monomers and a new bond vector $\mathbf{u}_1^{(j)}$ [or $\mathbf{u}_{N-1}^{(j)}$]. The bond vector is chosen to satisfy $\mathbf{u}_1^{(j)} \cdot \mathbf{u}_2^{(j)} \geq -0.5$ [or $\mathbf{u}_{N-1}^{(j)} \cdot \mathbf{u}_{N-2}^{(j)} \geq -0.5$], which prevents monomer $i = 1$ [or $i = N$] from backfolding onto monomer $i = 3$ [or $i = N-2$]. If accepted, the end monomer moves from $\mathbf{r}_1^{(j)}$ to $\mathbf{r}_1^{(j)} + \mathbf{u}_1^{(j)}$ [or from $\mathbf{r}_N^{(j)}$ to $\mathbf{r}_N^{(j)} - \mathbf{u}_{N-1}^{(j)}$] with all the other monomers shifting one bond along the chain contour (i.e., $\mathbf{r}_i^{(j)} \rightarrow \mathbf{r}_{i\pm1}^{(j)}$). Likewise, the end-rotation selects one of the $2n$ end monomers and a new bond vector, again with the same constraint that prevents backfolding for the reptation move. If accepted, the end monomer adopts the new bond vector while the rest of the chain remains fixed. The crankshaft trial selects one of the $(N-2)n$ middle monomers and an angle of rotation. If accepted, the middle monomer rotates about the axis connecting its two bonded neighbors. The swap trial randomly selects one of the stiff polymers, $j \in \{1, 2, ..., n_s\}$, and one of the flexible polymers, $j' \in \{n_s + 1, n_s + 2, ..., n\}$. If accepted, the two chains swap positions (i.e., $\mathbf{r}_i^{(j)} \leftrightarrow \mathbf{r}_i^{(j')}$).

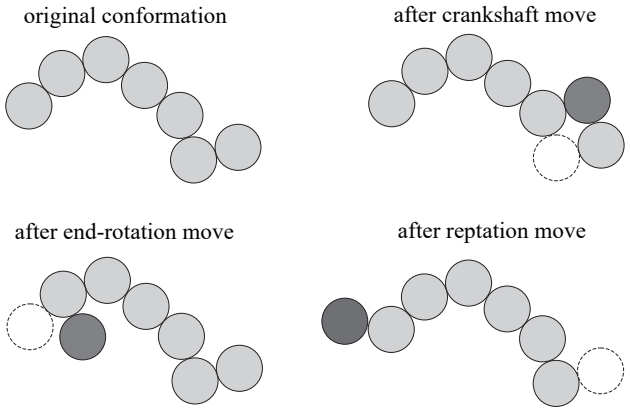


Figure 2: Illustrations of the three single-chain MC moves on an $N = 7$ chain. New monomer positions are denoted by dark circles and deleted monomer positions are indicated by dashed circles.

The efficiency of MC simulations is highly dependent on a judicious choice of MC moves.[24] Kumar and coworkers[16,17] only employed reptation, crankshaft, and swap trials. The acceptance rate of the reptation trial becomes small at high density, because of the difficulty in finding sufficient void space for a new position of the end monomer. The crankshaft trial has

a reasonable acceptance rate, but only because small-angle rotations require less void space. The acceptance rate of the swap move becomes particularly small when κ or N are large, due to the fact that the stiff chain must adopt $N-2$ new bond angles each characteristic of a flexible chain (i.e., $\kappa = 0$). The problem with a low acceptance of the reptation and swap trials is that this tends to pin the end monomers, since the crankshaft move only acts on middle monomers.[25] It is for this reason that we included the end-rotation trial, which maintains a reasonable acceptance rate for the same reason as the crankshaft trial. The acceptance rates for reptation, crankshaft, end-rotation, and swap moves were roughly 2–4%, 20–30%, 5–10%, and 0.004–40%, respectively, depending on the system parameters.

We start our simulations by placing equal numbers of flexible and stiff polymers between walls of cross-sectional area 10×10. This is done by randomly choosing the position of each first monomer, $\mathbf{r}_1^{(j)}$, and then the subsequent unit bond vectors, $\mathbf{u}_i^{(j)}$, subject to the constraint that all monomers must remain between the two walls. Given that the process is the same for both types of polymers, the simulations will necessarily begin with zero conformational asymmetry. Any overlaps between the monomers in the initial configuration will be gone once each monomer position has been renewed (i.e., has undergone a single move from Figure 2), which generally happens within 10^3 MC steps per monomer. Kumar and coworkers[17] generally terminated their equilibration at this point. Anything less is clearly insufficient, but even this number of MC steps is highly suspect given the general difficulty in equilibrating polymers of large N.[26,27] In particular, there is little time for the stiff polymers to evolve from their random-walk conformations to the more extended conformations corresponding to equilibrium, which could explain their underestimations of the conformational asymmetry between the stiff and flexible polymers (see Supplementary Information). Given the luxury of our faster MC moves, we continue the equilibration far beyond the first few seconds it now takes us to clear the overlaps. In fact, we extend the equilibration to approximately 10^9 MC steps per monomer. Following that, we periodically repeat the simulation box to produce a larger surface area, and equilibrate again for approximately 10^8 MC steps per monomer.

Once the equilibration is complete, we collect statistics for about 10^9 MC steps per monomer. Statistics are also collected for the smaller $10 \times 10 \times L_z$ boxes, to confirm that there are no significant finite-size effects. In contrast, Kumar et al. used from 10^8 to 5×10^8 MC moves to collect statistics on systems containing between 10^3 and 10^4 monomers (i.e., around 10^5 MC steps per monomer). Thus, we are able to perform roughly 10^4 times more MC steps. About two order of magnitude of this improvement can be attributed to the intervening 25 years of computer development. The remaining two orders can probably be attributed to our use of an efficient nearest-neighbor table. This is accomplished by dividing the simulation box into cells (or voxels). Because we are dealing with hard spheres, we able to choose the voxel size small enough (e.g., $0.5 \times 0.5 \times 0.5$) to limit the maximum occupancy to a single monomer (once the overlaps are gone), but large enough that a grid of only $5 \times 5 \times 5$ voxels needs to be checked for each single-chain move in Figure 2. With this innovation, we are able to perform approximately 10^8 MC steps per minute on a single CPU.

Results

Kumar et al. detected the segregation by sampling the distribution of monomer centers from the flexible and stiff polymers,

$$\hat{\rho}_f(z) = \frac{1}{L_x L_y} \sum_{i=1}^{N} \sum_{j=1}^{n_f} \delta(z - z_i^{(n_s+j)}) \tag{2}$$

$$\hat{\rho}_s(z) = \frac{1}{L_x L_y} \sum_{i=1}^{N} \sum_{j=1}^{n_s} \delta(z - z_i^{(j)}) \tag{3}$$

respectively, where $z_i^{(j)}$ is the z-component of the position vector $\mathbf{r}_i^{(j)}$. Their ensemble averages, $\rho_f(z)$ and $\rho_s(z)$, developed strong peaks at the surface due to layering. It is difficult to gauge the packing within the surface layers, because it depends on both the monomer concentration and the degree of localization (i.e., the width of the distribution). Given that the monomers are hard spheres, the physical volume occupied by the monomers is well defined.

Therefore, we instead examine the volume fractions of each monomer type,

$$\phi_\alpha(z) = \int \rho_\alpha(z - Z) H(1 - |\mathbf{R}|) d\mathbf{R} \tag{4}$$

which are bounded by a value of one. Here, $\alpha = s$ or f, $H(x)$ is the Heaviside function, and Z is the z-component of $\mathbf{R}$.

Our first simulation for $N = 40$ and $\kappa = 1$ starts with equal numbers of flexible and stiff polymers, $n_f = n_s = 24$, in a simulation box of size $10 \times 10 \times 32$. Because of a general tendency for flexible polymers to segregate to the surface, a depletion occurs in the bulk region. In our previous lattice simulations,[20] we tweaked the numbers of flexible and stiff polymers to restore the 50-50 composition in the bulk region, but this is challenging for the smaller system sizes typical of off-lattice simulations. For the current system size, the number of flexible polymers needs to be increased to 24.33, but of course n_f must be an integer. Fortunately, given the convenient fractional increase required, we were able to obtain an accurate balance by periodically repeating the simulation box three times in each lateral direction increasing its size to $30 \times 30 \times 32$ and then relabeling three of the stiff polymers as flexible polymers to obtain $n_f = 219$ and $n_s = 213$.

Figure 3 plots the distribution of the monomer centers, $\rho_f(z)$ and $\rho_s(z)$, as well as the concentration profiles, $\phi_f(z)$ and $\phi_s(z)$. The latter profiles exhibit strong peaks at $z \approx 0.8$ implying a well-defined layer of monomers with roughly equal populations from the flexible and stiff polymers. Despite the large 25% increase in concentration relative to the bulk concentration, the monomers remain loosely packed. The fact that $\phi_s(z)$ and $\phi_f(z)$ are both approximately 0.2 means that the average void space is approximately 60%, which is still rather large. Nevertheless, the total concentration of the layer is unrealistically large, given that even crystallization of a liquid does not generally increase concentration by more than 10%. This high compressibility implies that the monomer density chosen by Kumar et al., $nN/V = 0.6$, is still significantly less than that of a real melt.[20] There are also visible

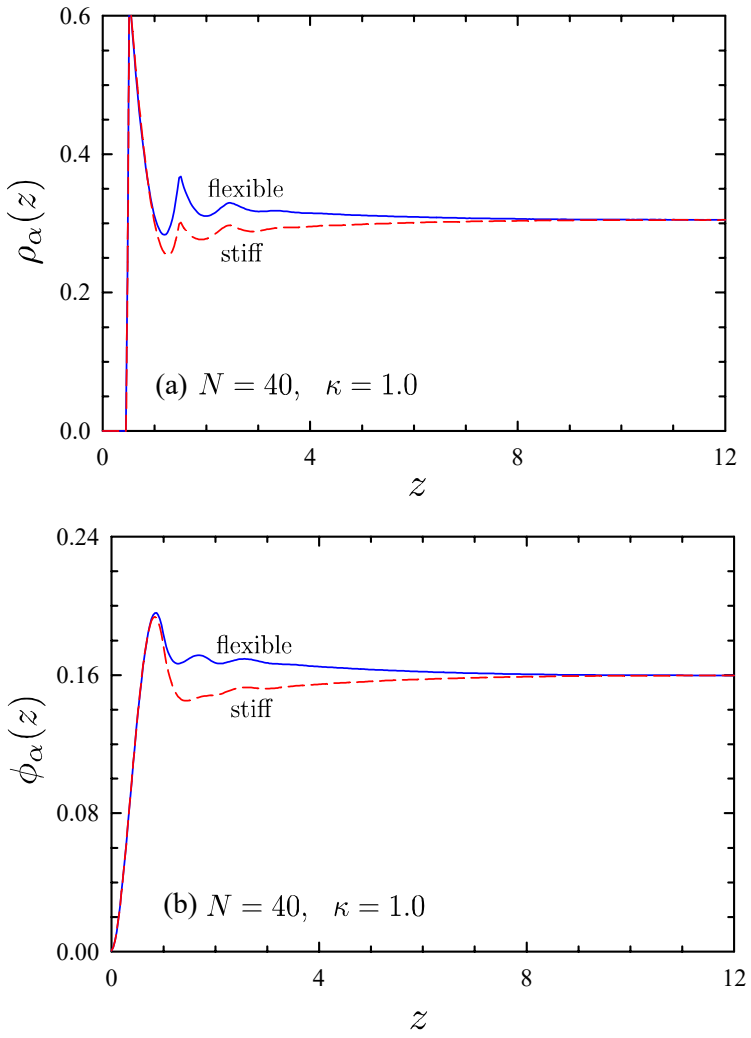


Figure 3: (a) Distribution of the monomer centers, $\rho_f(z)$ (solid curve), and stiff polymer, $\rho_s(z)$ (dashed curve), next to a hard wall, evaluated for equal polymerizations of $N = 40$ and a bending modulus of $\kappa = 1$ for the stiff polymers. (b) Analogous plots for the monomer concentrations, $\phi_f(z)$ and $\phi_s(z)$.

oscillations showing evidence for second and third layers, but in this case they are dominated by monomers from the flexible polymers.

We also examine the average end-to-end length of the flexible and stiff polymers, $R_{0,f}$ and $R_{0,s}$, respectively, which were obtained by sampling polymers in the bulk region. Note that the bulk is certain to remain in a mixed isotropic state for the small conformational asymmetries considered in our study.[20–22,28–30] From the end-to-end lengths, we evaluate the average

$$\bar{R}_0^2 \equiv (R_{0,f}^2 + R_{0,s}^2)/2 \tag{5}$$

which provides a scale for the conformational size of the polymers, and the ratio

$$\gamma \equiv R_{0,s}/R_{0,f} - 1 \geq 0 \tag{6}$$

which measures the conformational asymmetry. For the current value of $\kappa = 1$, the polymers have a conformational asymmetry of $\gamma = 0.13$. Even at this relatively small asymmetry (note that $0.2 \lesssim \gamma \lesssim 0.6$ in the experiments of Sikka et al.[7]), the amplitude of the segregation is 8% of the bulk concentration. Furthermore, this excess of flexible polymer persists well beyond the layering to a distance comparable to the average polymer size, $\bar{R}_0 = 9.08$.

Naturally, the required increase in n_f to achieve a 50-50 bulk composition is rarely a convenient fraction, and so for the rest of the simulations we choose to just double the system in the lateral directions without adjusting n_f. The parameters used for the remaining simulations are listed in Table 1. Even though we keep $n_f = n_s$, the system sizes are sufficiently large that the bulk concentrations, $\phi_{0,\alpha}$, do not deviate far from 0.5. For instance, the simulations for $N = 40$ and $\kappa = 1$ with $n_f = n_s = 96$ result in bulk concentrations of $\phi_{0,f} = 0.493$ and $\phi_{0,s} = 0.507$. In any case, the definition of surface excess of flexible polymer

$$\phi_{\rm ex}(z) = (\phi_f(z) - \phi_s(s) - \phi_{0,f} + \phi_{0,s})/2 \tag{7}$$

accounts for the asymmetry in composition (i.e., $\phi_{\rm ex}(z) \to 0$ as $z \to \infty$). Although $\phi_{\rm ex}(z)$ will still depend on the bulk composition to some degree, the effect is negligible for the systems in Table 1. Indeed, the $\phi_{\rm ex}(z)$ obtained from the concentration profiles in Figure 2(b) is virtually identical to the one obtained for $n_f = n_s = 96$.

Table 1: Parameters for the simulations in Figures 4 and 5.

N	κ	n_s	n_f	$L_x \times L_y \times L_z$	$\bar{R}_0$	γ
40	0.5	96	96	$20 \times 20 \times 32$	8.72	0.05
40	1.0	96	96	$20 \times 20 \times 32$	9.08	0.12
40	1.5	96	96	$20 \times 20 \times 32$	9.54	0.21
40	2.0	96	96	$20 \times 20 \times 32$	10.10	0.32
20	1.0	144	144	$20 \times 20 \times 24$	6.18	0.14
80	1.0	72	72	$20 \times 20 \times 40$	12.82	0.13
160	1.0	48	48	$20 \times 20 \times 64$	18.84	0.12

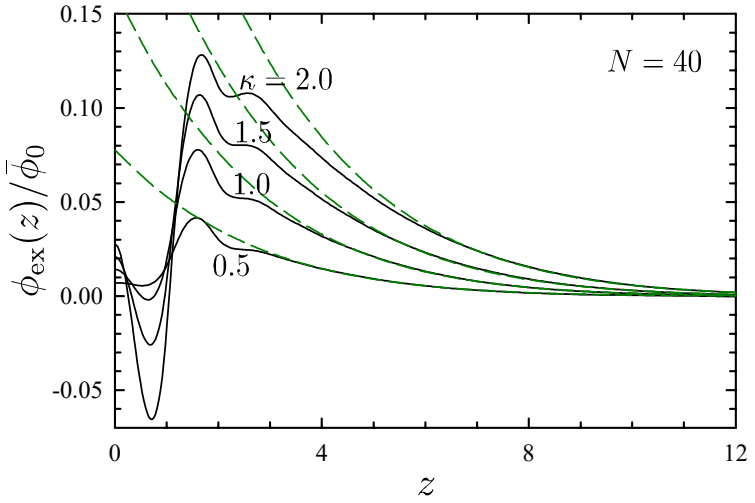


Figure 4: Excess of flexible polymer, $\phi_{\rm ex}(z)$, relative to the average bulk concentration, $\bar{\phi}_0 \equiv (\phi_{0,f} + \phi_{0,s})/2$, evaluated for a fixed polymerization of $N = 40$ and a range of different bending moduli, κ. The dashed curves are fits to $\phi_{\rm ex}(z) = A_\rho F_\rho(Z)$.

Figure 4 compares the excess of flexible polymer, $\phi_{\rm ex}(z)$, as the bending modulus of the stiff polymer, κ, is increased. As expected, the amplitude of the excess increases due to the increasing conformational asymmetry: $\gamma = 0.05$, 0.12, 0.21, and 0.32 for $\kappa = 0.5$, 1.0, 1.5, and 2.0, respectively. Although the stiff polymer tends to dominate the first layer of monomers ($z \approx 0.8$) as κ increases, the total (i.e., integrated) excess is always dominated by

the flexible polymer. The range of the excess remains relatively constant, as expected given that there is only a small variation in $\bar{R}_0$ (see Table 1). Particularly remarkable is the fact that the excess of flexible polymer beyond the layering quantitatively matches the profile

$$F_\rho(Z) = \frac{(1+Z^2)}{\sqrt{\pi}} \exp(-Z^2) - \left(\frac{3Z}{2} + Z^3\right) \mathrm{erfc}(Z) \tag{8}$$

predicted by Wu et al.,[15] where $Z = \sqrt{3/2}z/\bar{R}_0$. The dashed curves in Figure 4 denote the fits $\phi_{\mathrm{ex}}(z) = A_\rho F_\rho(Z)$, where the amplitude, A_ρ, is the only fitting parameter.

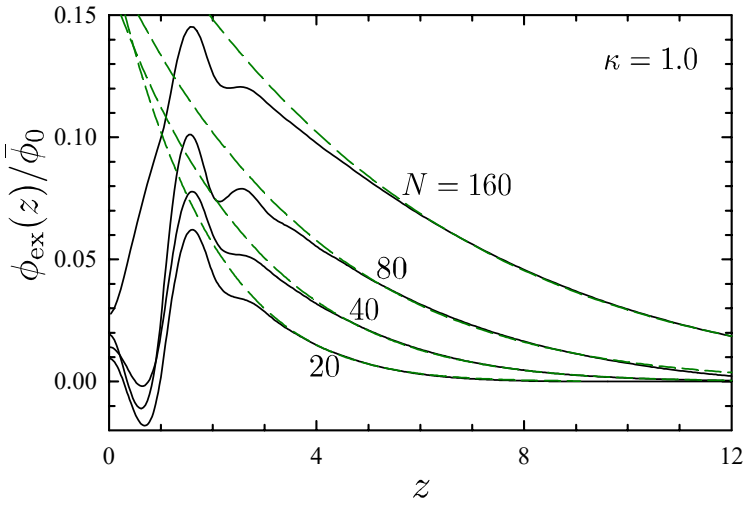


Figure 5: Analogous plots to those of Figure 4, but evaluated for a fixed $\kappa = 1$ and a range of different N.

Figure 5 performs a similar comparison, but this time for blends with increasing polymerizations, N, where the bending modulus of the stiff polymer is fixed at $\kappa = 1$. As expected, the range of the excess increases as the polymers become larger; $\bar{R}_0 = 6.2$, 9.1, 12.8, and 18.8 for $N = 20$, 40, 80, and 160, respectively. In this case, the conformational asymmetry, γ, is relatively independent of N as it should be, unlike the erratic dependence reported by Kumar et al. (see Supporting Information). Again, the single-parameter fits to $\phi_{\mathrm{ex}}(z) = A_\rho F_\rho(Z)$ agree well the long-range excesses. Furthermore, the magnitude of the excess increases as the polymers become larger, which is qualitatively consistent with the SCFT calculations of Wu et al.[15] This can be attributed to the fact that larger polymers

have more conformational entropy.

Discussion

Our findings are in stark contrast to those of Kumar et al.[16,17] While we observed a long-range excess of flexible polymers extending to $z \sim \bar{R}_0$, they reported a short-range excess of stiff polymers only extending to $z \sim 1$. Direct comparisons are provided in the Supporting Information, where we repeat four of their simulations using identical parameter values. The differences are most severe for the larger polymers, but they still remain significant even for their shortest $N = 10$ polymer. The inconsistency is readily explained by a lack of equilibration as initially suspected[20] as well as a lack of statistics. We performed many orders of magnitude more equilibration and several orders of magnitude more statistics. The mere fact that we get distinctly different results is enough to prove that they did not perform enough MC steps, assuming the computer codes are free of errors. To ensure that our longer durations were sufficient, however, we monitored the size of the molecules, $R_{0,f}$ and $R_{0,s}$, the bending energy of the stiff polymers, $U_{\rm bend}$, and the symmetry of the concentration profiles, $\phi_\alpha(z) - \phi_\alpha(L_z - z)$. The excess concentration, $\phi_{\rm ex}(z)$, was the slowest quantity to equilibrate, much more so than the time required for the initial value of $\gamma = 0$ to reach its equilibrium. Indeed, Kumar et al. obtained values of γ for $N = 10$ and 25 that are only slightly smaller than ours, and yet their profiles remained inaccurate. For $N = 50$ and 100, however, it appears that they did not wait long enough for γ to equilibrate.

We generally ran our simulations several times longer than necessary, to be certain that the statistical inaccuracies were within the line widths of our plots. The two exceptions were for $N = 80$ and 160. To obtain accurate results for these longer polymers in a reasonable amount of time (i.e., on the order of a month), we combined 20 and 30 independent runs, respectively. Based on the statistical variation in the independent runs, the uncertainty in those results is about twice the line widths in Figure 5. Even though there is a clear

explanation for why the previous simulations differed from ours, we performed a battery of tests to ensure that our simulations were free of errors. This included comparing our efficient algorithm against a slow but very basic version of the code, and running simulations with different combinations of MC moves (i.e., reptation+swaps, end-rotation+crankshaft+swaps, reptation+end-rotation+crankshaft, and just reptation). We also snipped polymers in half and confirmed that the equilibrated concentration profiles for N evolved into those for $N/2$, illustrating that our results were independent of how the system was initialized. Furthermore, the close quantitative agreement with eq (8) in Figures 4 and 5 is too improbable to be a mere coincidence, and thus we can be confident that there are no errors in our simulations and that they are as accurate as claimed.

The quantitative agreement that we observe between the long-range part of $\phi_{\rm ex}(z)$ in the simulations and the $F_\rho(Z)$ derived from SCFT is particularly significant, given that the simulations are for the hard tangent-sphere model whereas the derivation is for the continuous Gaussian-chain model. This was also the case in our previous lattice simulations,[20] which implies that $F_\rho(Z)$ is universal to all models. If so, then it must also be universal to all experiments, since models can always be refined to provide an arbitrarily accurate representation of any experimental system. The derivation of $F_\rho(Z)$ does, however, assume small conformational asymmetry,[15] and indeed the fits to $\phi_{\rm ex}(z) = A_\rho F_\rho(Z)$ become less accurate for large κ (see Figure 4), as was the case for the lattice simulations in ref 20. The applicability of the derivation also relies on large N, although $F_\rho(Z)$ still remains surprisingly accurate for polymers as short as $N = 20$ (see Figure 5). We note that an analogous universality has been predicted for entropic segregation due to size disparity,[3,4] and likewise confirmed by simulations.[5]

The SCFT calculation by Wu et al.[15] was performed by splicing together a short-range profile near the surface with the long-range profile in eq (8). Although the outer profile is evidently universal, the inner solution depends on the details of the system. As a consequence, the amplitude of the outer profile, A_ρ, cannot possibly be universal. Indeed, this

was illustrated in our previous study of the lattice model, where simulations were performed with difference surface fields.[20] Now that we have shown $F_\rho(Z)$ to be a universal profile, the next issue will be to understand how the inner solution and thus A_ρ depends on the system details, including packing effects. However, this is beyond the scope of the present paper.

Our new simulation results have serious implications for a number of previous works. First of all, they contradict the short-range excess of stiff polymer predicted by the wall-PRISM calculations of Kumar et al.[16,17] While wall-PRISM undoubtedly accounts for the local correlations near the wall, its closure relation may restrict its ability to treat the long-range correlations relevant to the outer solution. The wall version of PRISM also has a number of addition approximations that could be faulty. Donley et al.[31] have argued that wall-PRISM and thus the simulations of Kumar et al.[16,17] are consistent with the SCFT calculation of Wu et al.[15] as well as the experiments of Sikka et al.[7,8] This too must be incorrect, and indeed we have identified subtle logical flaws that negate their arguments (see Supporting Information). Lastly, the fluctuation-corrected calculation of Stepanow and Fedorentko[18] is now inconsistent with all available simulations. This may be due to their choice of boundary condition for the effective single-chain Green's function; they considered Dirichlet and Neumann (reflecting) boundary conditions, choosing the latter, but they overlooked the Robin (mixed) boundary condition suggested by the SCFT calculation of Wu et al.[15]

Given the extreme increase in MC steps required to correct the results by Kumar et al.,[16,17] there are a few other simulations from the same time period that may have to be reconsidered. In particular, there are some by Weinhold et al.[28] for long polymers of $N = 200$. We also have concerns regarding simulations of an analogous tangent-sphere model;[25,32] although the monomers in that model were slightly penetrable, the simulations were performed at higher density with similarly long polymers. Yethiraj[23] considered entropic segregation of much smaller $N = 19$ polymers, but some of his excess concentrations extend well beyond $\bar{R}_0$, the limit implied by the universal profile. Given that, one might even wonder about

several other simulations involving similarly sized polymers.[33–36] The later simulations may have benefited from a 'jiggling' MC move where all the monomers of a chain underwent small random displacements, but this was also true of the simulations in ref 23.

Conclusions

In summary, we have shown that the number of MC steps used in the previous off-lattice simulations by Kumar and coworkers[16,17] was insufficient. To obtain accurate results, we increased the equilibration and statistics by multiple orders of magnitude, which resolved their erratic behavior in conformational asymmetry, γ (see Supplementary Material). More importantly, the improved equilibration and statistics reversed the simulation results. The initial simulations reported a general surface excess of stiff polymers with a range that only extended about one monomer diameter into the melt regardless of the polymerization. Our more accurate simulations, on the other hand, find an integrated excess of flexible polymers with a range that tracks the average size of the polymers.

Given this revelation, the literature now becomes consistent with a general entropic surface preference for polymers of short statistical segment length. This suggests that packing effects are not critically important and that the previous experimental results[7–11] can, in fact, be attributed to entropic segregation. Although the bulk of the literature is now consistent, it is markedly inconsistent with the wall-PRISM calculations of Kumar et al.[16,17] and the fluctuation corrections to SCFT by Stepanow and Fedorentko.[18]

It is particularly significant that the tail of the excess conforms to the profile in eq (8) predicted by Wu et al.[15] for small degrees of conformational asymmetry. The fact that the profile shape, $F_\rho(Z)$, was predicted for continuous Gaussian chains and that it quantitatively agreed with our off-lattice simulations as well as our previous lattice simulations[20] implies that it is a universal result that applies to all models as well as all experiments. The next challenge will be to understand what properties control the amplitude, A_ρ, of the profile.

Supporting Information

Direct comparisons to previous simulations by Kumar et al.[17] and issues with related discussion by Donley et al.[31] The data supporting the findings of this study and the computer code are available from the authors upon reasonable request.

Acknowledgments

The authors are grateful for useful discussions with James Donley and Marcus Müller. Computational resources were provided by Compute Canada.

References

(1) Binder, K. Surface effects on polymer blends and block copolymer melts: Theoretical concepts of surface enrichment, surface induced phase separation and ordering. *Acta Polymerica* **1995**, *46*, 204–225.

(2) Hariharan, A.; Kumar, S. K.; Russell, T. P. A lattice model for the surface segregation of polymer chains due to molecular weight effects. *Macromolecules* **1990**, *23*, 3584–3592.

(3) Minnikanti, V. S.; Qian, Z.; Archer, L. A. Surface segregation and surface tension of polydisperse polymer melts. *J. Chem. Phys.* **2007**, *126*, 144905.

(4) Mahmoudi, P.; Matsen, M. W. Entropic segregation of short polymers to the surface of a polydisperse melt. *Euro. Phys. J. E* **2017**, *40*, 86.

(5) Mahmoudi, P.; Forrest, W.; Beardsley, T. M.; Matsen, M. W. Testing the universality of entropic segregation at polymer surfaces.*Macromolecules* **2018**, *51*, 1242–1247.

(6) Hill, J. A.; Endres, K. J.; Mahmoudi, P.; Matsen, M. W.; Wesdemiotis, C.; Foster, M. D.

Detection of Surface Enrichment Driven by Molecular Weight Disparity in Virtually Monodisperse Polymers. *ACS Macro Lett.* **2018**, *7*, 487–492.

(7) Sikka, M.; Singh, N.; Karim, A.; Bates, F. S.; Satija, S. K.; Majkrzak, C. F. Entropy-driven surface segregation in block copolymer melts. *Phys. Rev. Lett.* **1993**, *70*, 307–310.

(8) Sikka, M.; Singh, N.; Bates, F. S.; Karim, A.; Satija, S.; Majkrzak, C. F. Surface segregation in model symmetric polyolefin diblock copolymer melts. *J. Phys. II France* **1994**, *4*, 2231–2248.

(9) Scheffold, F.; Budkowski, A.; Steiner, U.; Eiser, E.; Klein, J.; Fetters, L. J. Surface Phase Behavior in Binary Polymer Mixtures. II. Surface Enrichment from Polyolefin Blends. *J. Chem. Phys.* **1996**, *104*, 8795–8806.

(10) Tretinnikov, O. N.; Ohta, K. Surface Segregation in Stereochemically Asymmetric Polymer Blends. *Langmuir* **1998**, *14*, 915–920.

(11) Tretinnikov, O. N. Surface Segregation in Polymer Blends of Minimal Difference in the Components Surface Energy. *Macromol. Symp.* **2000**, *149*, 269–275.

(12) Fredrickson, G. H.; Donley, J. P. Influence of broken conformational symmetry on the surface enrichment of polymer blends. *J. Chem. Phys.* **1992**, *97*, 8941–8946.

(13) Tripathi, S.; Chapman, W. G. Microstructure and Thermodynamics of Inhomogeneous Polymer Blends and Solutions. *Phys. Rev. Lett.* **2005**, *94*, 087801.

(14) Donley, J. P.; Fredrickson, G. H. Influence of Conformational Asymmetry on the Surface Enrichment of Polymer Blends II. *J. Polym. Sci. Part B* **1995**, *33*, 1343–1351.

(15) Wu, D. T.; Fredrickson, G. H.; Carton, J.-P. Surface Segregation in Conformationally Asymmetric Polymer Blends: Incompressibility and Boundary Conditions. *J. Chem. Phys.* **1996**, *104*, 6387–6397.

(16) Yethiraj, A.; Kumar, S.; Hariharan, A.; Schweizer, K. S. Surface segregation in polymer blends due to stiffness disparity. *J. Chem. Phys.* **1994**, *100*, 4691–4694.

(17) Kumar, S. K.; Yethiraj, A.; Schweizer, K. S.; Leermakers, F. A. M. The effects of local stiffness disparity on the surface segregation from binary polymer blends. *J. Chem. Phys.* **1995**, *103*, 10332–10346.

(18) Stepanow, S.; Fedorentko, A. A. Surface Segregation of Conformationally Asymmetric Polymer Blends. *Phys. Rev. E* **2006**, *73*, 031801.

(19) Nikoubashman, A.; Register, R. A.; Panagiotopoulous, A. Z. Sequential Domain Realignment Driven by Conformational Asymmetry in Block Copolymer Thin Films. *Macromolecules* **2014**, *47* 1193–1198.

(20) Spencer, R. W. K.; Matsen, M. W. Surface Segregation in Athermal Polymer Blends due to Conformational Asymmetry. *Macromolecules* **2021** *54*, 10100–10109.

(21) Ivanov, V. A.; Rodionova, A. S.; Martemyanova, J. A.; Stukan, M. R.; Müller, M.; Paul, W.; Binder, K. Wall-induced orientational order in athermal semidilute solutions of semiflexible polymers: Monte Carlo simulations of a lattice model. *J. Chem. Phys.* **2013**, *138*, 234903.

(22) Ivanov, V. A.; Rodionova, A. S.; Martemyanova, J. A.; Stukan, M. R.; Müller, M.; Paul, W.; Binder, K. Conformational Properties of Semiflexible Chains at Nematic Ordering Transitions in Thin Films: A Monte Carlo Simulation. *Macromolecules* **2014**, *47*, 1206–1220.

(23) Yethiraj, A. Entropic and Enthalpic Surface Segregation from Blends of Branched and Linear Polymers. *Phys. Rev. Lett.* **1995**, *74*, 2018–2021.

(24) Wolfgardt, M.; Baschnagel, J.; Binder, K. Monte-Carlo Simulations of 3–Dimensional

Glassy Polymer Melts: Reptation Versus Single Monomer Dynamics *J. Phys. II France* **1995**, *5*, 1035–1052.

(25) Kumar, S. K.; Vacatello, M.; Yoon, D. Y. Off-lattice Monte Carlo simulations of polymer melts confined between two plates. *J. Chem. Phys.* **1988**, *89*, 5206–5215.

(26) Hsu, H.-P.; Kremer, K. Efficient equilibration of confined and free-standing films of highly entangled polymer melts. *J. Chem. Phys.* **2020**, *153*, 144902.

(27) Luca Tubiana, L.; Kobayashi, H.; Potestio, R.; Dünweg, B.; Kremer, K.; Virnau, P.; Daoulas, K. Comparing equilibration schemes of high-molecular-weight polymer melts with topological indicators. *J. Phys.: Condens. Matter* **2021**, 204003.

(28) Weinhold, J. D.; Kumar, S. K.; Singh, C.; Schweizer, K. S. Athermal stiffness blends: A comparison of Monte Carlo simulations and integral equation theory. *J. Chem. Phys.* **1995**, *103*, 9450–9474.

(29) Kozuch, D. J.; Zhang, W.; Milner, S. T. Predicting the Flory-Huggins χ Parameter for Polymers with Stiffness Mismatch from Molecular Dynamics Simulations. *Polymers*, **2016**, *8*, 241.

(30) Milchev, A.; Egorov, S. A.; Midya, J.; Binder, K.; Nikoubashman, A. Entropic Unmixing in Nematic Blends of Semiflexible Polymers. *ACS Macro Lett.*, **2020**, *9*, 1779–1784.

(31) Donley, J. P.; Wu, D. T.; Fredrickson, G. H. On the Control of Surface Enrichment in Polymer Blends and Copolymers. *Macromolecules* **1997** *30*, 2167–2174.

(32) Kumar, S. K.; Vacatello, M.; Yoon, D. Y. Off-lattice Monte Carlo simulations of polymer melts confined between two plates. 2. Effects of chain length and plate separation. *Macromolecules* **1990**, *23*, 2189–2197.

(33) Dickman, R.; Hall, C. K. High density Monte Carlo simulations of chain molecules:

Bulk equation of state and density profile near walls. *J. Chem. Phys.* **1988**, *89*, 3168–3174.

(34) Yethiraj, A.; Hall, C. K. Monte Carlo simulations of hard chain–hard sphere mixtures in slitlike pores. *J. Chem. Phys.* **1989**, *91*, 4827–4837.

(35) Yethiraj, A.; Hall, C. K. Monte-Carlo simulation of polymers confined between flat plates. *Macromolecules* **1990**, *23*, 1865–1872.

(36) Yethiraj, A. Effect of chain stiffness on the conformational properties, pair correlations, and equation of state of polymer melts. *J. Chem. Phys.* **1994**, *101*, 9104–9112.